Strength Enhancement of Prestressed Concrete Dapped-End Girders

Dr.Shatha Dhia Mohammed
Lecturer
College of Engineering- University of Baghdad
Email:Shathadhia@yahoo.com

Dr. Thamer Khudair Mahmoud
Professor
College of Engineering- University of Baghdad
Email:thamir.azawi@gmail.com

ABSTRACT

This paper presents the application of nonlinear finite element models in the analysis of dapped-ends pre-stressed reinforced concrete girders under static loading by using ANSYS software. The girder dimensions are (4.90 m span, 0.40 m depth, 0.20 m width, 0.20 m nib depth, and 0.10 m nib length) and the parameters considered in this research are the pre-stress effect, and strand profile (straight and draped).

The numerical results are compared with the experimental results of the same girders. The comparisons are carried out in terms of initial prestress effect, load- deflection curve, and failure load. Good agreement was obtained between the analytical and experimental results. Even that, the numerical model was stiffer than the experimental, but; there were a good agreements in both trends and values. The difference varies in the range (5-12)% for the deflection. Results have shown that the pre-stress force has increased the static ultimate load capacity by (35%) in case of straight strand and by (97%) in case of draped strand

Key words: dapped-end girder, finite element, prestress.

تعزيز مقاومة الروافد الخرسانية المسبقة الجهد ذات النهايات المستدقة

شذى ضياء محمد
مدرس
كلية الهندسة - جامعة بغداد

د.ثامر خضير محمود
استاذ
كلية الهندسة - جامعة بغداد

الخلاصة

يقدم هذا البحث دراسة التحليل الغير خطي باستخدام نظرية العناصر المحددة لتحليل العتبات الخرسانية المسبقة الجهد ذات النهايات المستدقة تحت تاثير الاحمال الاستاتيكية باستخدام برنامج (ANSYS). ابعاد العتب المحلل كانت (4.90 م للفضاء, 0.40 م عمق , 0.20 م عرض , 0.20 م عمق النهاية المستدقة و 0.10 م طول النهاية المستدقة) . قام البحث بدراسة تاثير كل منذ قوة الاجهاد و مسار حبال الشد (مستقيمة , منحنية) على التحمل الاقصى للعتب .

تمت مقارنة النتائج العددية مع ما يماثلها من نتائج عملية وقد كانت المقارنة بدلالة الانحناء الاولي الناتج عن قوة الشد , منحني القوة-الهطول و حمل الفشل وقد اظهرت المقارنة تقاربا جيدا بين النتائج النظرية و مثيلاتها العملية. وعلى الرغم من كون النموذج الممثل باستخدام نظرية العناصر المحددة كان اكثر جساءة من مثيله عمليا الا ان النتائج اظهرت توافقا جيدا من ناحيتي النزعة والقيم القصوى تتراوح بين (5-12)%. كما وجد بان قوة الاجهاد المسبق تزيد من مقدار الحمل الاقصى بنسبة (35%) لحالات حبال الشد ذات المسار المستقيم و بنسبة (97%) لحالات المسار المنحني.

الكلمات الرئيسية: الروافد ذات النهايات المستدقة, العناصر المحددة, الاجهاد المسبق

1. INTRODUCTION

The severe stress concentration at the re-entrant corner of the dapped- end girders, due to unusual shape, didn't restrict the extensively using of such girders in different types of structures. It is a better choice for better lateral stability; since it lowers the deck center of gravity by indentation supporting corbel into the depth of the supported girders. The re-entrant corner, certainly, can be considered as the weakest location in the dapped-ends girder. It requires special details of reinforcement, otherwise, a rapid diagonal tension cracks may propagate and a failure will acquire with few or no warning.

Many of researches had been started since 1969 when Reynold, **Reynold, G. C., 1969,** developed suitable reinforcement details evolving a design procedure for dapped-end members. Then after many researches were made to study the shear capacity and behavior of RC dapped-end beams, **Ajina, J. M., 1986, Herzinger, R. and El-Badry, M. M. ,2002, Liem, S. K., 1983, Mohamed, R. N. and Elliott, K. S., 2008, Reynold, G. C., 1969, Wang, Q. , Guo, Z. and Hoogenboom, P.C.J., 2005**. PCI, ACI and STM design method were considered to detect the most sufficient and economic design of dapped-end beam, **Ahmed, S. et al, 2013, Barton, D. L., 1988, Huang, P.C, J.J Myers and A. Nanni, 2000, Mader, B. S., 1999, Mattock, A. H., and Theryo, T., 1986** . There were also many researches that studied the effect of different reinforcement details on the response of dapped-end beam, **Herzinger, R. and El-Badry, M. M. ,2002, Mattock, A. H., and Theryo, T., 1986**. The effect of geometric layout of the dapped- end (nib height and width) were also considered in some researches, **Chung, J. C. J, 1985, Khan, M. A., 1981**.

2. FINITE ELEMENT TYPES CONSIDERED IN THE PRESENT STUDY

The concrete will be modeled using Solid65 element. This element has eight nodes with three degrees of freedom at each node (translations in the nodal x, y, and z directions). Plastic deformation, cracking in three orthogonal directions, and crushing are the most important capability of this element that made it a suitable choice to model concrete material. **Fig. 1** shows the schematic drawing of this element.

Steel reinforcement and steel strand are modelled using Link8 element. This element is a 3D spar element and it has two nodes with three degrees of freedom at each node (translations in the nodal *x*, y and z directions) as shown in **Fig. 2**. This element is also capable to represent an initial strain and plastic deformation at high stress level.

The Solid45 element is used for modelling the steel plates at the supports and loading locations to prevent stress concentration and to provide stress distribution over supports and loading areas. The element is defined with eight nodes having three degrees of freedom at each node – translations in the nodal x, y, and z directions. The geometry and node locations for this element type are shown in **Fig. 3**.

3. MATERIAL PROPERTIES

The required parameters to identify the material models are listed in **Table 1**. Regarding Solid65 element (set No. 1), the model includes density, linear isotropic and multi-linear isotropic properties to properly model concrete material. The compressive uniaxial stress-strain relationship for the concrete model (multi-linear isotropic) was obtained using the following equations, **MacGregor, 1992.**

$$f = \frac{E_c \varepsilon}{1+\left(\frac{\varepsilon}{\varepsilon_o}\right)^2} \quad (1)$$

$$\varepsilon_o = \frac{2f_c'}{E_c} \quad (2)$$

$$E = \frac{f}{\varepsilon} \quad (3)$$

Where:
f = Stress at any strain.
ε = Strain at stress f.
ε_o = Strain at the ultimate compressive strength fc'.
E = Modulus of elasticity.

Based on Hook's law and Eq. (1), the adopted stress-strain relationship for concrete used in this study, **Fig. 4 (b)** was that as suggested by **Jindal, A., 2012, Wolanski, B. S., 2001, and Kachlakev, D. I., 2005**. The curves start at zero stress and strain while the first points (defined at 0.3 fc') was calculated in the linear range, Eq. (3). The rest points (2-6) were calculated from Eq. (1) with ε_o obtained from Eq. (2).

Model numbers 2, and 3 refer to Link8 element. This element was used for all steel reinforcement and it is assumed to be bilinear isotropic behavior at nonlinear stage. Bilinear isotropic material is also based on the Von Mises failure criteria. This model requires the yield stress (f_y), as well as the hardening modulus of the steel to be defined.

Material model number 4 refers to the Solid45 element used for the steel plates at loading points and at supports. Therefore, this element is modeled as a linear isotropic element.

Material model number 5 represents the properties of pre-stressing steel. It was modeled as multilinear isotropic material following the von Mises failure criteria. The pre-stressing steel was modeled using a multilinear stress-strain curve developed using the following equations, **Wolanski, B. S.,2001.**

$$\varepsilon_{ps} \leq 0.008\ ; \quad f_{ps} = 28\,000\ \varepsilon_{ps}\ ksi \tag{4}$$

$$\varepsilon_{ps} > 0.008\ ; \quad f_{ps} = 286 - \frac{0.075}{(\varepsilon_{ps} - 0.0065)} < 0.98 f_{ps}\ ksi \tag{5}$$

4. GEOMETRY AND FINITE ELEMENT MODELING

Three simply supported dapped-ends girders that had the same geometric layout, flexural and shear reinforcement (**Fig. 5, Fig. 6 and Table 2)** are analyzed using ANSYS finite elements model. All the tested beams were designed, according to PCI Design Handbook 6th Edition [16] requirements to fail at their ends.

The dapped-ends girders, anchorages, load plates, and support plates were modeled as volumes. The combined volumes are shown in **Fig.7** for both straight and draped strand profiles, respectively, while the layout of the generated draped duct is sown in **Fig. 8**.

The use of a rectangular or square mesh is recommended for Solid65 element to obtain good results, **Wolanski, B. S., 2001**. However, the presence of the duct, reduces the possibility to mesh the circular hole properly. Therefore, finer the mesh was set for elements as possible near the duct. The overall mesh of the concrete, load and support plate volumes is shown in **Fig. 9** for the straight and draped strands, respectively. Lines were created so that they pass through the nodes of the reinforcement bars, then after a mesh line command was adopted to generate the reinforcement elements. However, the necessary mesh attributes as described above need to be set before each section of the reinforcement is created. **Fig. 10 and Fig. 11** show the overall mesh of the steel reinforcement for a straight and draped strands, respectively.

5. VALIDATION OF THE FINITE ELEMENT MODEL

In order to validate the finite element modeling of reinforced and prestressed dapped-ends concrete beams , the finite element model using ANSYS program has been applied to analyze a compatible concrete beams tested in by **Mohammed, S. D., and Mahmoud, T. K., 2014**. The predicted results are compared with the experimental results. The comparison includes prestress effect, load-deflection relation, and failure load.

5.1 Pre-stress effect

The deflections obtained from experimental work **(Mohammed, S. D., and Mahmoud, T. K., 2014)**, hand calculations, and from the FE analysis due to the pre-stress effect are given in **Table 3** (no hand calculation was considered for cases of draped strand profile). **Fig. 12** shows the deflected shape due to pre-stress effect for each tested specimens. From **Table 3** it is clear that there is a good agreement between the experimental, hand calculations. The difference varies between (1%) and (6%).

5.2 Load - deflection relation.

The results obtained from the FE analysis for the load – deflection relation are presented in **Fig. 13** while **Fig.14** shows the contour lines of the deflection at the failure stage. The presentation also includes a comparison between the experimental **(Mohammed, S. D., and Mahmoud, T. K., 2014)** and numerical results. Even that the numerical models were stiffer than the experimental, but; there were a good agreement in both trend and amplitude that varies between (5%) and (12%).

5.3 Load at failure

In the finite element analysis, the continuity in the solution process, depends on the concepts of rigid body motion. The small load increment solution continues until there is a dis-converge in results. **Table 4** gives the failure load as obtained from the FE analysis and the experimental work **(Mohammed, S. D., and Mahmoud, T. K., 2014)** for each modeled specimens.

6. RESPONSE AND BEHAVIOUR OF DAPPED-END REINFORCEMENT

Five positions were adopted to get better understanding for the response and behaviour of the dapped-end reinforcement that is recommended by the PCI**, PCI Design Handbook 6th Edition 2004,** as shown in **Fig. 15**. The effect of the pre-stressing presses was investigated, **Fig. 16** shows the advantage of the draped strand profile on the response of shear and flexure reinforcement (A_h, A_v, A_s, A_{sh}, and $A_{s'h}$) It is clear that in case of draped strand, the reinforcement yields when approaching the failure stage which indicates a good strengthening for the concrete.

The crack patterns, for each modeled specimen, as obtained from ANSYS program are shown in **Fig.17**. These cracks were selected at the failure stage. It is clear that the initial crack generated at the re-entrant corner of the dapped-ends girder and extends then after toward the applied load. This is compatible with the experiment test results by **Mohammed, S. D., and Mahmoud, T. K., 2014**.

7. CONCLUSIONS

Based on the predicted results from the finite element analysis, the following conclusions may be drown:

1. There was no significant difference in the effect of pre-stress force, for both straight and draped strand profile, on the response of flexural reinforcement (A_s, A_h, and $A_{s'h}$) up to crack

stage. Then after the strain load curves show a separation due to the stiffening effect of draped pre-stress force.

2. The behavior and response of shear reinforcement (A_v and A_{sh}) under the effect of straight and draped strand profile are similar to that of flexural reinforcement of the dapped-ends girder.

3. Straight pre-stress profile shows about (35%) more effect on the response of shear reinforcement (A_{sh}) than other types of shear reinforcement (A_v).

4. A similar crack pattern in all specimens was detected. Cracks started with the initiation of diagonal re-entrant crack, followed by nib inclined crack and diagonal tension crack (developed in the full-depth of the girder).

5. The general behavior of the finite element model presented by the load- deflection shows a good agreement in both trend and amplitude.

6. The finite element model behavior was stiffer than that of the tested specimen due to the effect of bond slip between the concrete and steel bars and the effect of micro cracks which were excluded in the finite element analysis. The overestimation in the failure load as calculated by the finite element analysis was (4-11)%.

REFERENCE

- Ahmed, S. et al, 2013, *Evaluation of the Shear Strength of Dapped Ended Beam*, Life Science Journal, Vol. 10, No. 3, PP. 1038-1044.

- Ajina, J. M., 1986, *Effect of Steel Fibers on Precast Dapped-End Beam*, CMS Thesis, South Dakota State University, Brookings, SD.

- Barton, D. L., 1988, *Detailing of Structural Concrete Dapped End Beams*, MS Thesis, University of Texas at Austin, Austin, TX.

- Chung, J. C-J, 1985, *Effect of Depth of Nib on Strength of a Dapped-End Beam*, MS Thesis, University of Weshington, Seattle, WA.

- Herzinger, R. , El-Badry, M. M. ,2002, *Use of Stud Shear Reinforcement in Concrete Beams with Dapped Ends*, 4th Structural Specialty Conference of the Canadian Society for Civil Engineering, Montréal, Québec, Canada 5-8 June 2002 .

- Huang, P.C, J.J Myers and A. Nanni, 2000, *Dapped-End Strengthening in Precast Prestressed Concrete Double Tee Beams with FRP Composites*, Proc., 3rd Inter. Conf. on Advanced Composite Materials in Bridges and Structures, Ottawa, Canada, J. Humar and A.G. Razaqpur, Editors, 15-18 Aug. 2000, pp. 545-552.

- Jindal, A., 2012, *Finite Element Modeling of Reinforced Concrete Exterior Beam-Column Joint Retrofitted with Externally Bonded Fiber Reinforced Polymer (FRP)*, M.Sc. Thesis, Thapar University, Patiala, India.
- Kachlakev, D. I., 2005, *Finite Element Analysis and Model Validation of Shear Deficient Reinforced Concrete Beams Strengthened With GFRP Laminates*, California Polytechnic State University.

- Khan, M. A., 1981, *A Study of the Behavior of Reinforced Concrete Dapped-End Beams*, M. Sc Thesis, University of Washington, Seattle, WA, PP. 145.

- Liem, S. K., 1983, *Maximum Shear Strength of dapped-End or corbel*, MS Thesis, Concordia University, Montreal, Quebec, Canada.

- Mader, B. S., 1999, *Detailing Dapped Ends of Pretensioned Concrete Beams*, MS. Thesis, University of Texas at Austin, Austin, TX.

- MacGregor, J. G., 1992, *Reinforced Concrete Mechanics and Design*, Prentice-Hall, Inc., Englewood Cliffs, NJ, PP 848.

- Mattock, A. H., and Theryo, T., 1986, *Strength of Members with Dapped Ends*, PCI Research Project No. 6, Final Report, Precast/Prestressed Concrete Institute, Chicago, IL.

- Mohamed, R. N. and Elliott, K. S., 2008, *Shear Strength of Short Recess Precast Dapped end Beams Made of Steel Fiber Self-Compacting Concrete*, 33rd Conference on OUR WORLD IN CONCRETE & STRUCTURES: 25 – 27 August 2008, Singapore.

- Mohammed, S. D., and Mahmoud, T. K., 2014. *Effect of Prestress Force on the Strength of Dapped-End Reinforced Concrete Beams*, ACCMES Conference, June 2014 (Japan).

- PCI, 2004, *PCI Design Handbook - Precast and Prestressed Concrete*, Sixth Edition, Precast/Prestressed Concrete Instituted, Chicago, Illinois.

- Reynold, G. C., 1969, *The Strength of Half-Joints in Reinforced Concrete Beams*, TRA 415, Cement and Concrete Association, London, United Kingdom, June, PP. 9.

- Wang, Q. , Guo, Z. and Hoogenboom, P.C.J., 2005, *Experimental Investigation on the Shear Capacity of RC Dapped end Beams and Design Recommendations*, Structural Engineering and Mechanics, Vol. 21, No. 2, PP. 221- 235.

- Wolanski, B. S., 2001, *Flexural Behavior of Reinforced and Pre-Stressed Beam Using Finite Element Analysis*, M. Sc. Thesis, Marquette University.

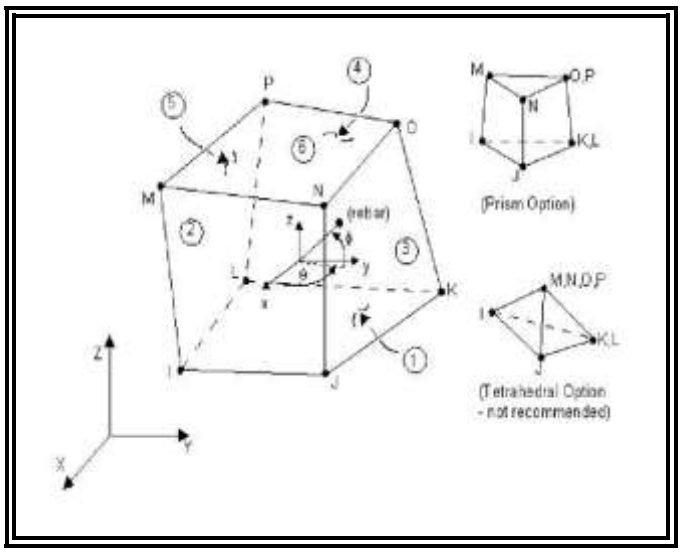

Figure 1. Solid65 element (ANSYS help, 2009).

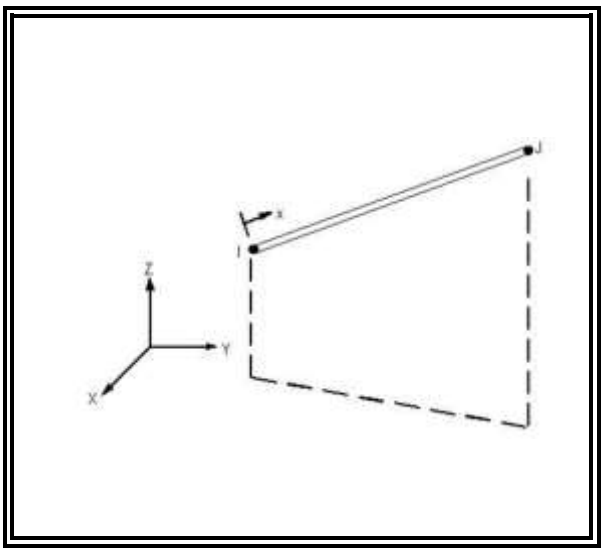

Figure 2. Link8 element (ANSYS help, 2009).

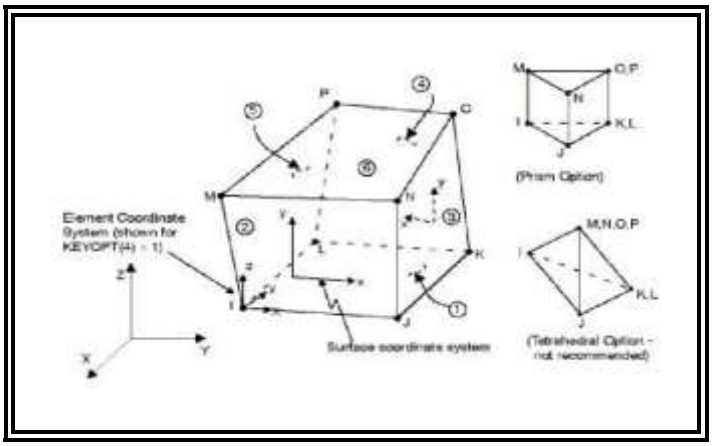

Figure 3. Solid45 element (ANSYS help, 2009).

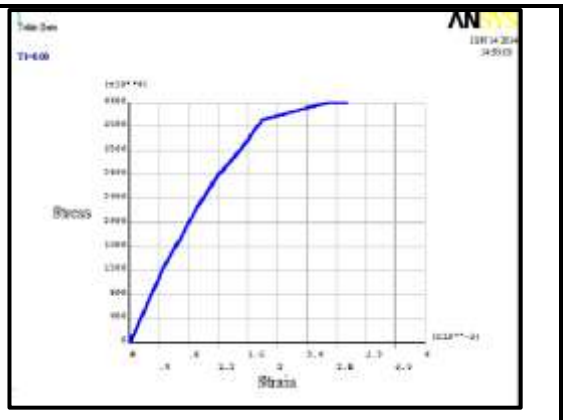

a- Uniaxial stress-strain curve of concrete.

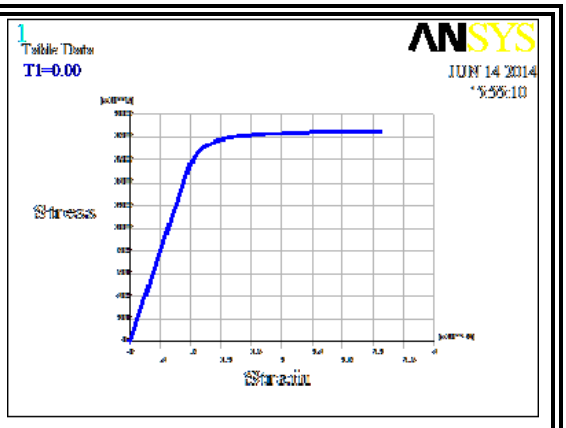

b- Stress-strain curve of 270 Ksi strand

Figure 4. Stress-strain curve for (a- concrete & b- strand).

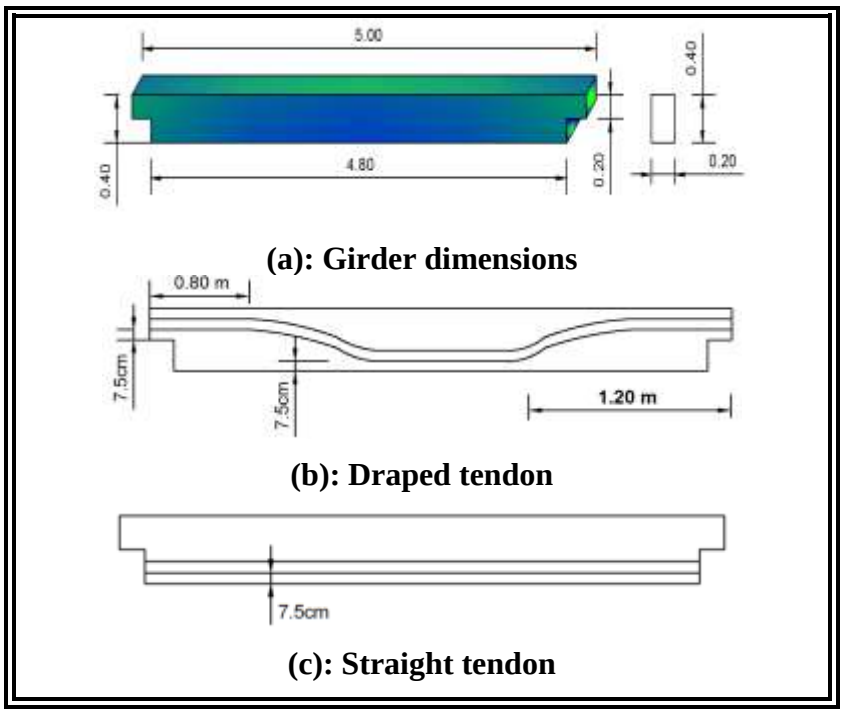

Figure 5. Geometric layout of the modeled girder (Mohammed, S. D., and Mahmoud, T. K., 2014).

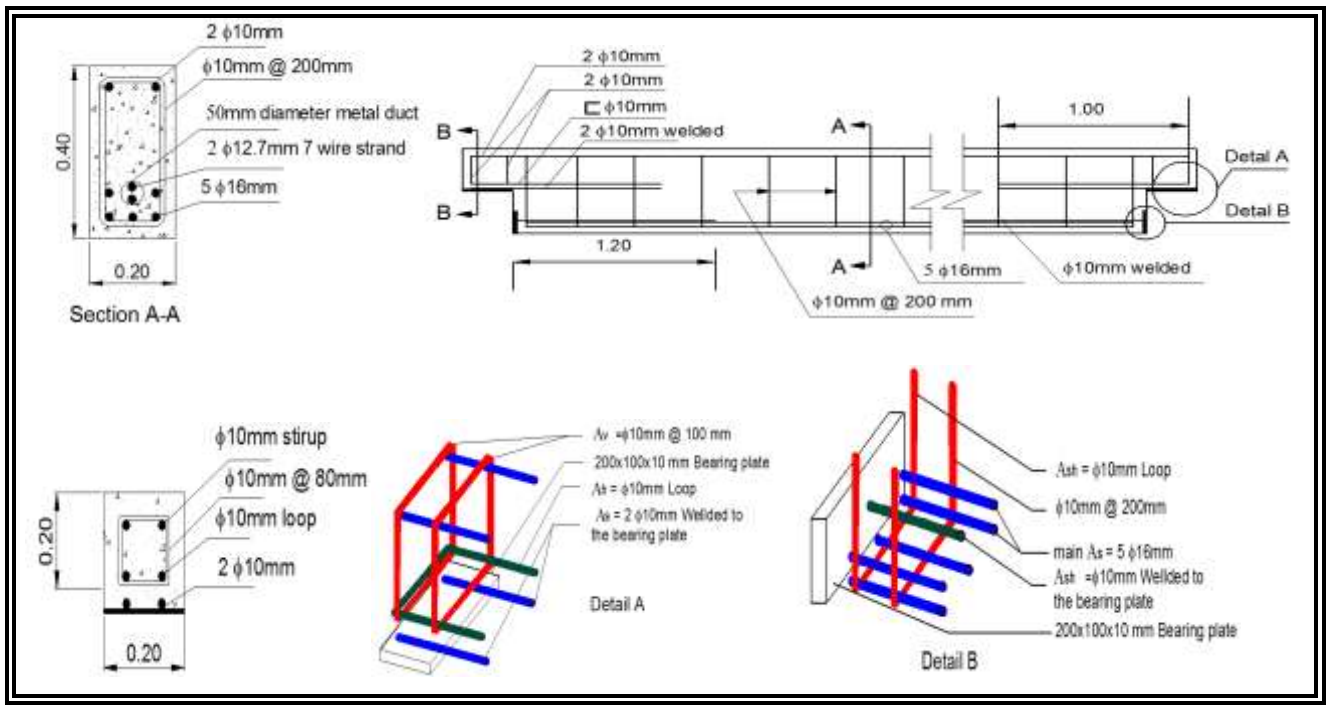

Figure 6. Details of the reinforcement (Mohammed, S. D., and Mahmoud, T. K., 2014).

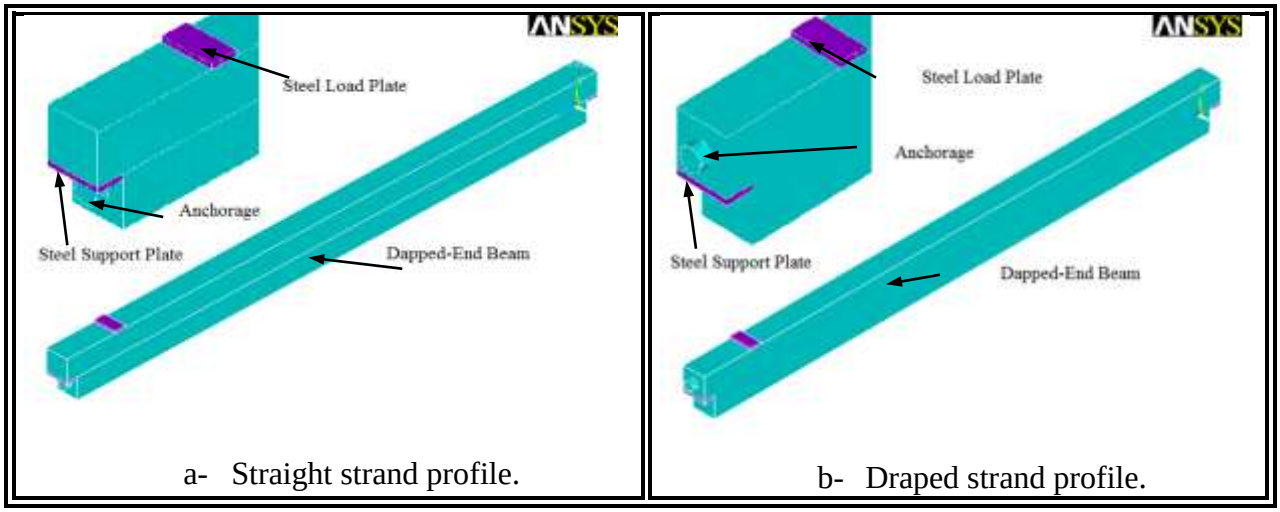

a- Straight strand profile. b- Draped strand profile.

Figure 7. Volumes of the modeled dapped-ends girder.

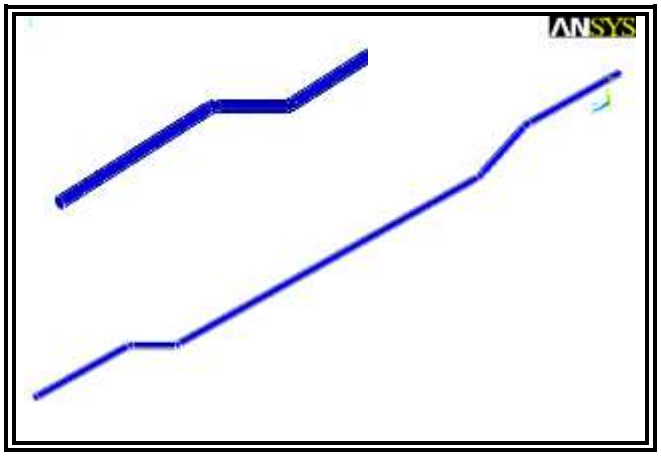

Figure 8. Volumes created for draped duct**.**

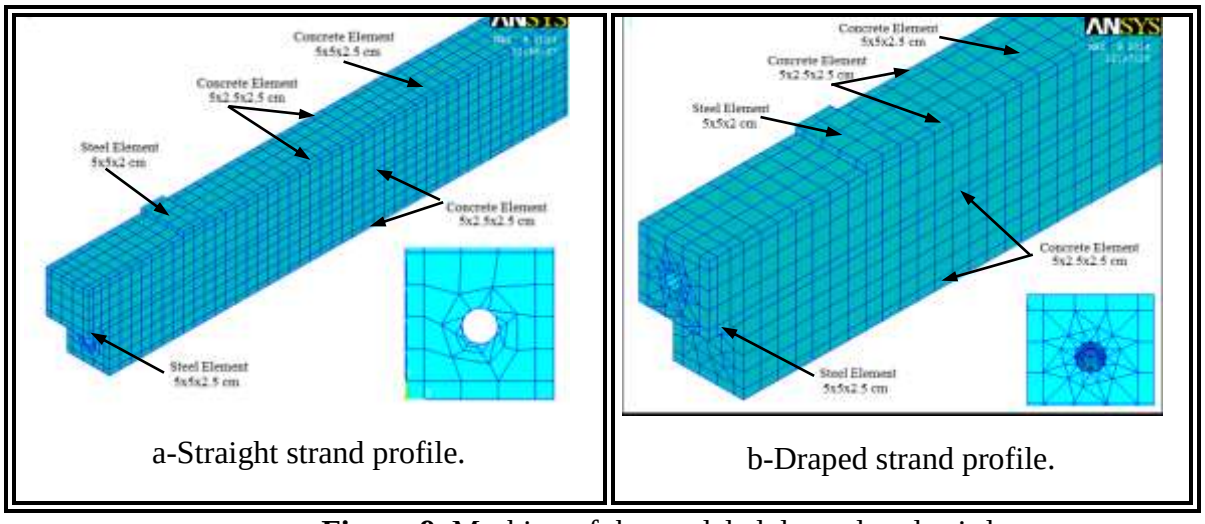

a-Straight strand profile. b-Draped strand profile.

Figure 9. Meshing of the modeled dapped-ends girder

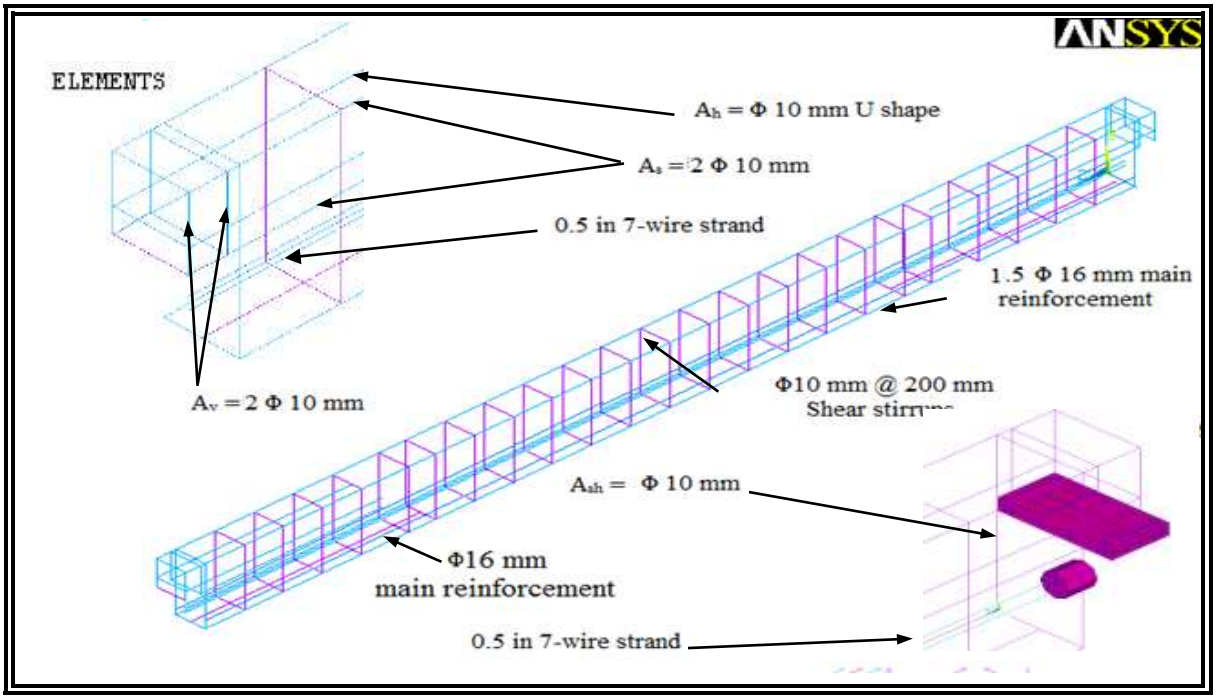

Figure 10. Reinforcement configuration for straight strand profile.

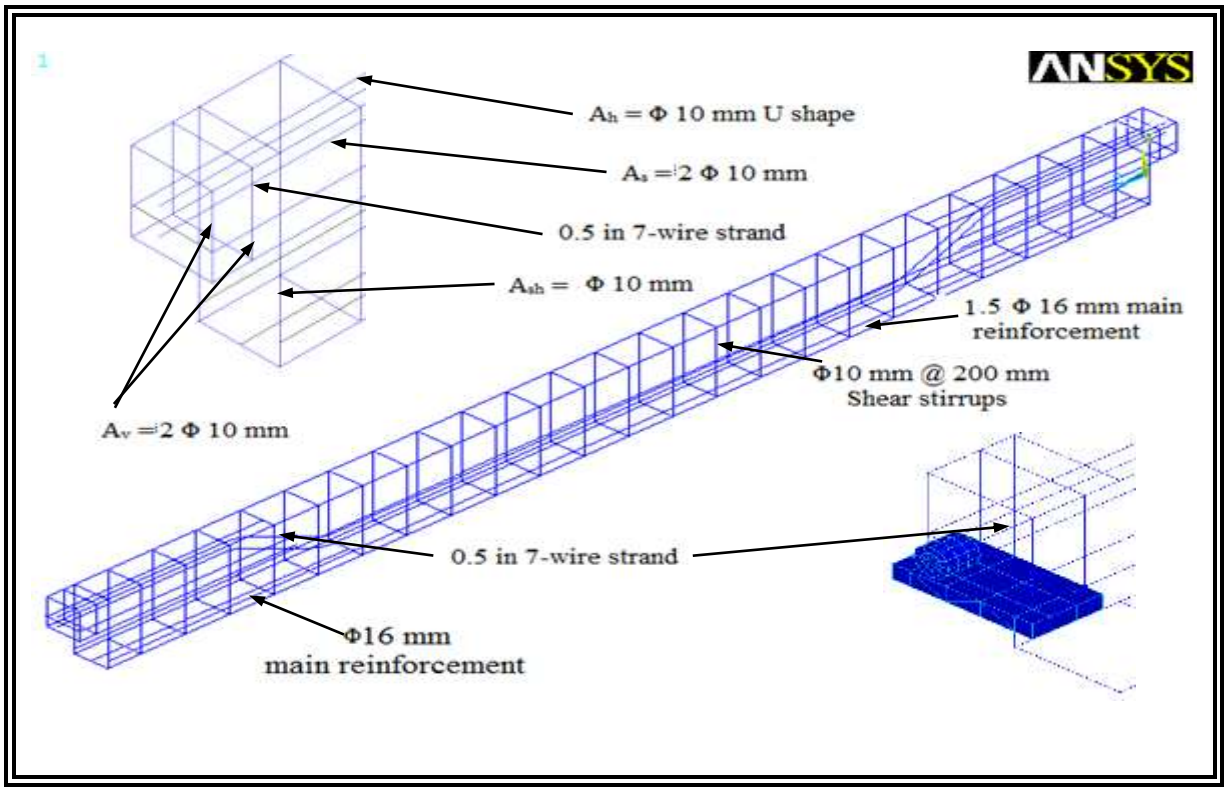

Figure 11. Reinforcement configuration for draped strand profile.

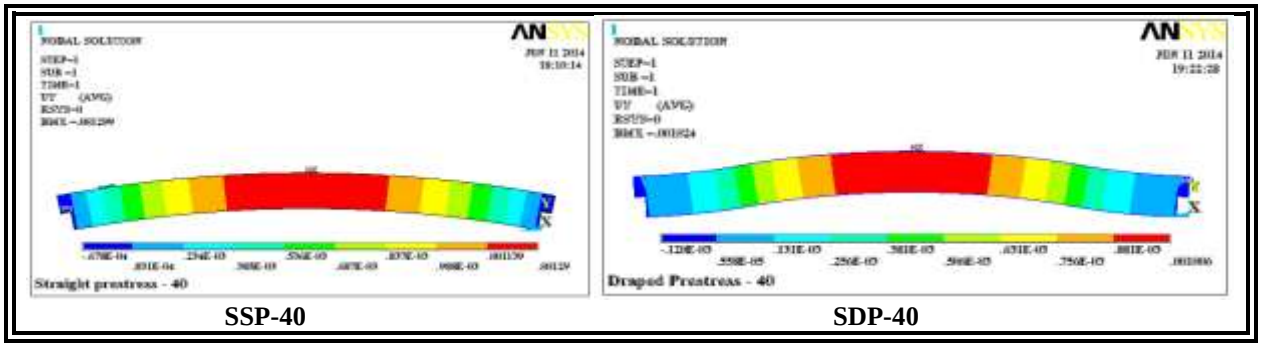

Figure 12. Contour of the pre-stress effect

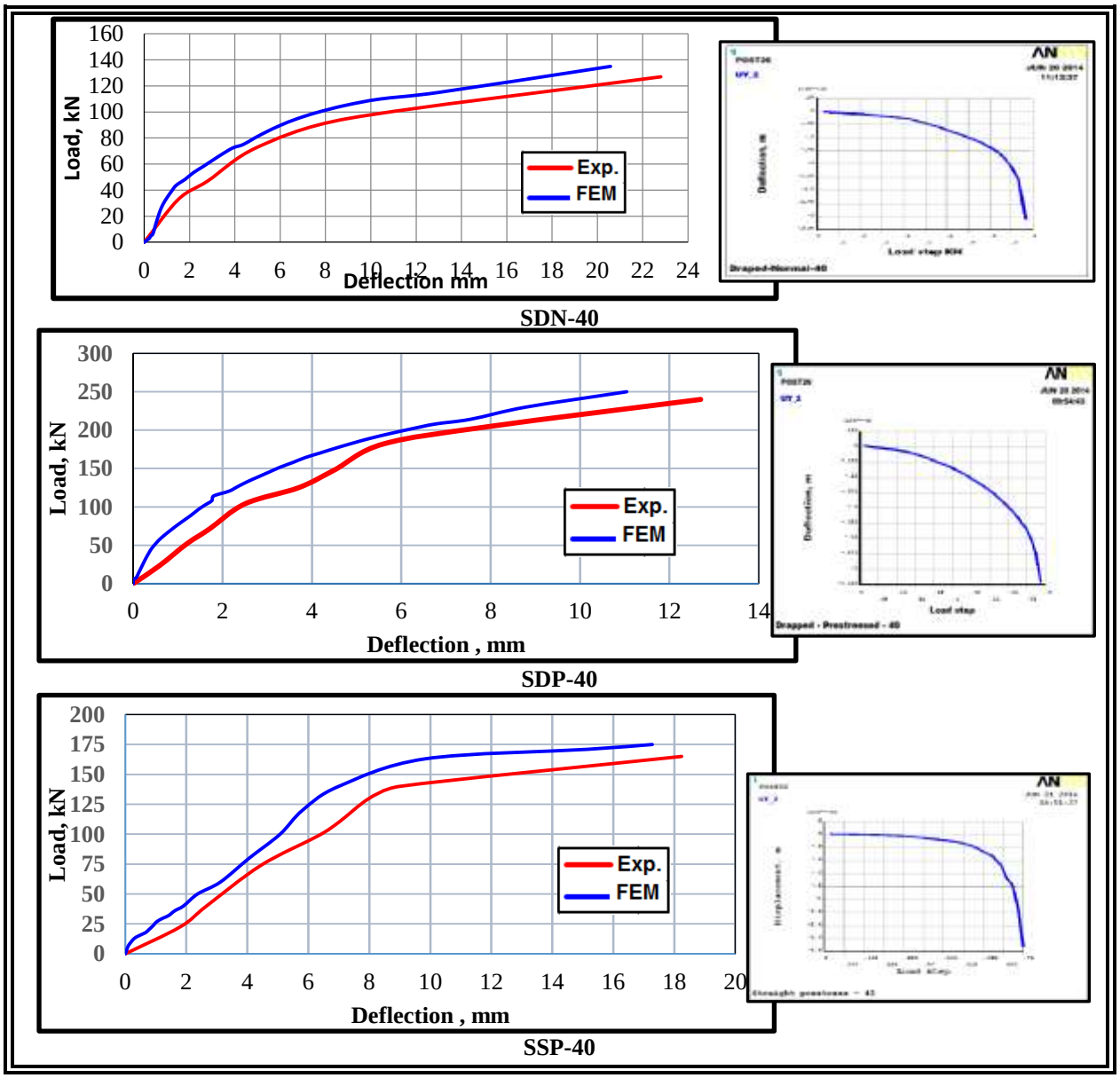

Figure 13. Comparison of load-deflection relation.

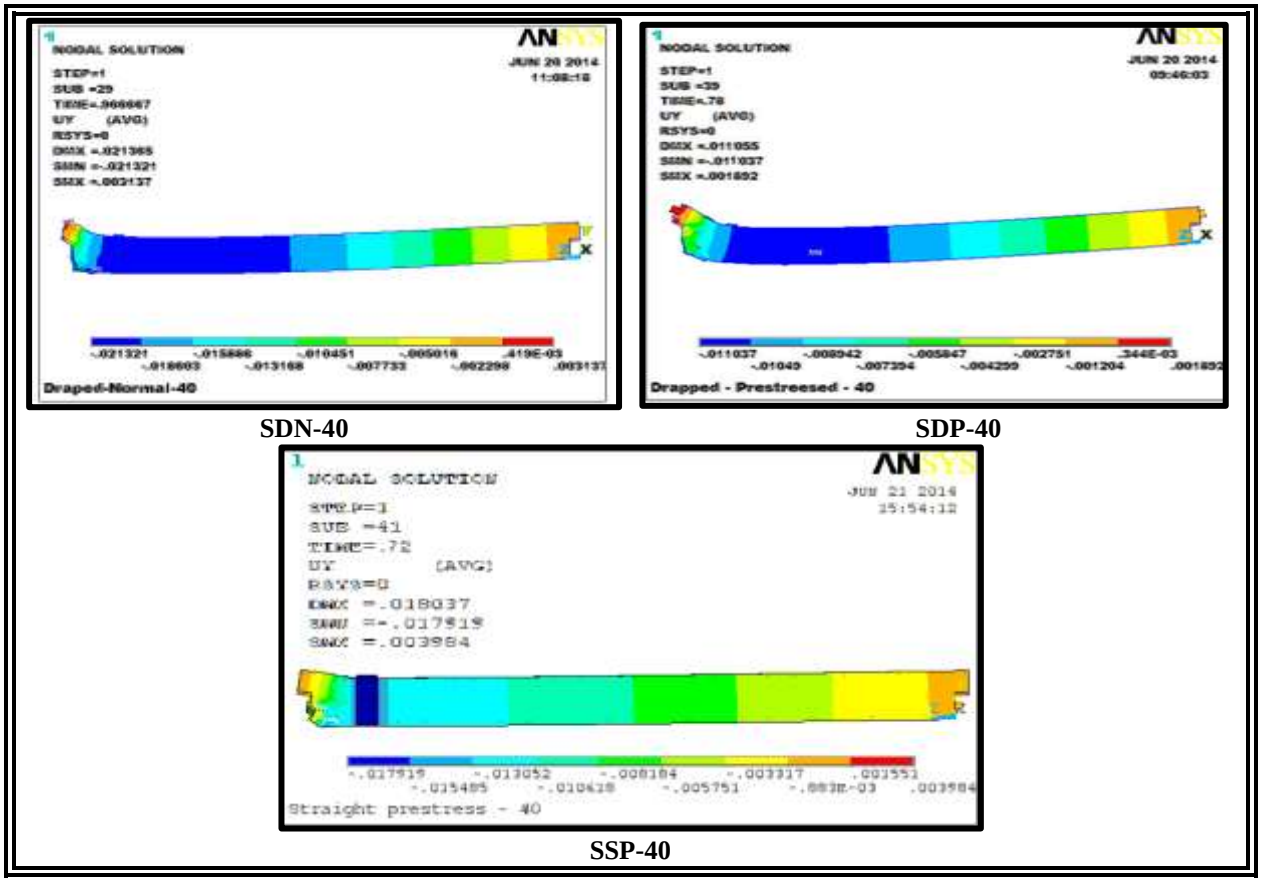

SDN-40 **SDP-40**

SSP-40

Figure 14. Deflection contour at failure stage.

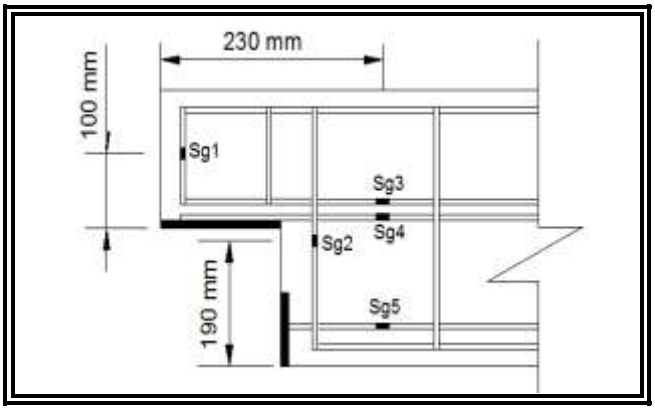

Figure 15. Adopted locations on the dapped-end reinforcements.

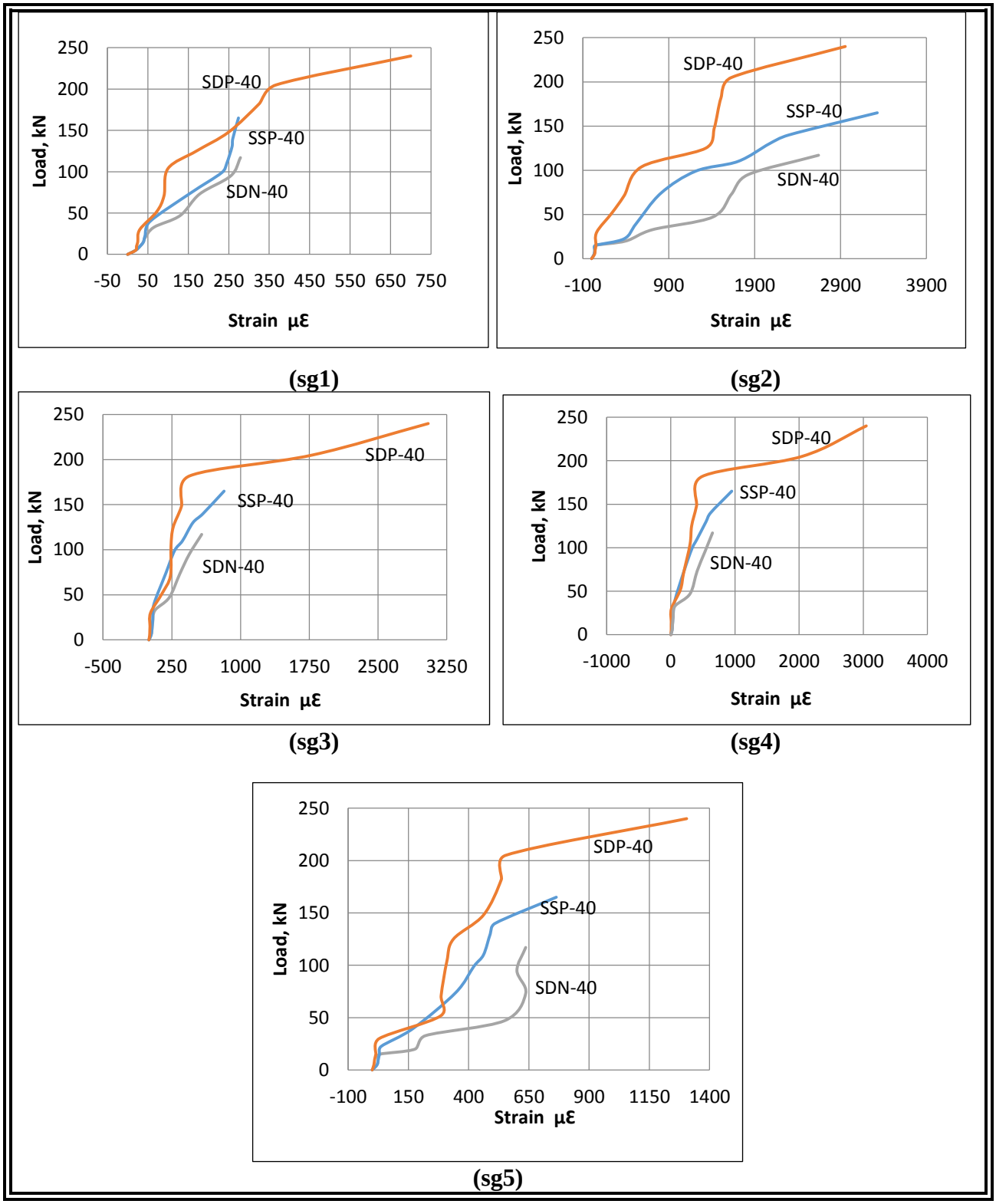

Figure 16. Load – strain curve at different locations.

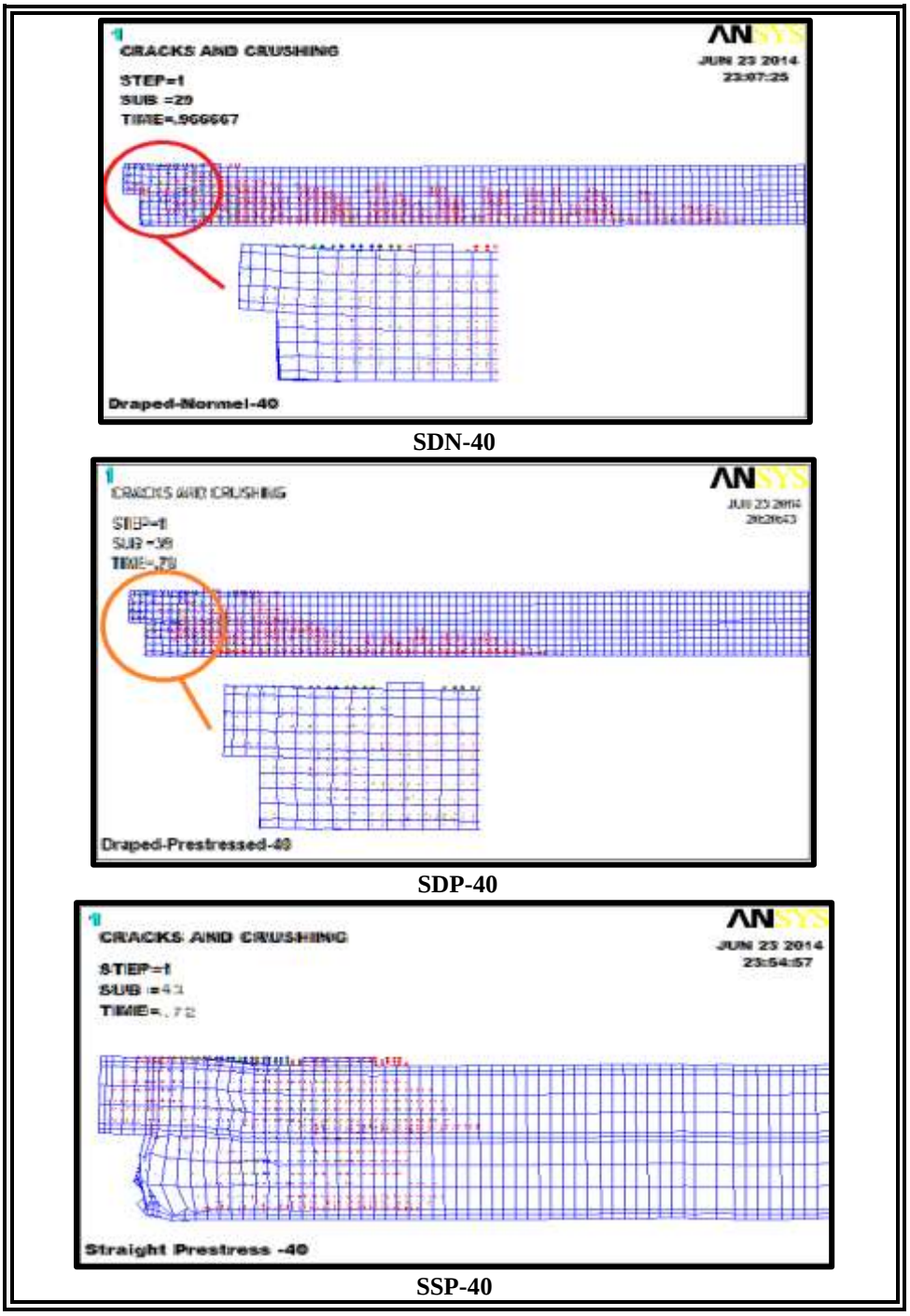

Figure 17. Crack pattern at failure stage.

Table 1. Material properties.

<table>
<tr><th>Material Model NO.</th><th>Element Type</th><th>Material Properties</th></tr>
<tr><td>1</td><td>Solid65</td><td>
<table>
<tr><th colspan="2">Linear Isotropic</th></tr>
<tr><td>EX</td><td>29725 MPa</td></tr>
<tr><td>PRXY</td><td>0.2</td></tr>
</table>
<table>
<tr><th>Density</th></tr>
<tr><td>2500 kg</td></tr>
</table>
<table>
<tr><th colspan="2">Multilinear Isotropic</th></tr>
<tr><td>Strain</td><td>Stress MPa</td></tr>
<tr><td>0.0004</td><td>12.00</td></tr>
<tr><td>0.0006</td><td>16.99</td></tr>
<tr><td>0.009</td><td>24.06</td></tr>
<tr><td>0.0012</td><td>29.76</td></tr>
<tr><td>0.00185</td><td>36.97</td></tr>
<tr><td>0.002</td><td>38.30</td></tr>
<tr><td>0.00269</td><td>39.98</td></tr>
</table>
<table>
<tr><th colspan="2">Concrete</th></tr>
<tr><td>ShrCf-Op</td><td>0.2</td></tr>
<tr><td>ShrCf-Cl</td><td>0.8</td></tr>
<tr><td>UnTensSt</td><td>4.0 MPa</td></tr>
<tr><td>UnCompSt</td><td>40 MPa</td></tr>
<tr><td>BiCompSt</td><td>0</td></tr>
<tr><td>HydroPrs</td><td>0</td></tr>
<tr><td>BiCompSt</td><td>0</td></tr>
<tr><td>UnTensSt</td><td>0</td></tr>
<tr><td>TenCrFac</td><td>0</td></tr>
</table>
</td></tr>
<tr><td>2</td><td>Link 8</td><td>
<table>
<tr><th colspan="2">Linear Isotropic</th></tr>
<tr><td>EX</td><td>200000 MPa</td></tr>
<tr><td>PRXY</td><td>0.3</td></tr>
</table>
<table>
<tr><th colspan="2">Bilinear Isotropic</th></tr>
<tr><td>Yield stress</td><td>630MPa</td></tr>
<tr><td>Tangent modulus</td><td>0</td></tr>
</table>
</td></tr>
<tr><td>3</td><td>Link 8</td><td>
<table>
<tr><th colspan="2">Linear Isotropic</th></tr>
<tr><td>EX</td><td>200000 MPa</td></tr>
<tr><td>PRXY</td><td>0.3</td></tr>
</table>
<table>
<tr><th colspan="2">Bilinear Isotropic</th></tr>
<tr><td>Yield stress</td><td>593MPa</td></tr>
<tr><td>Tangent modulus</td><td>0</td></tr>
</table>
</td></tr>
<tr><td>4</td><td>Solid 45</td><td>
<table>
<tr><th colspan="2">Linear Isotropic</th></tr>
<tr><td>EX</td><td>200000 MPa</td></tr>
<tr><td>PRXY</td><td>0.3</td></tr>
</table>
</td></tr>
</table>

Table 2. Details of the modeled girders.

Girder No.	$f_{c'}$ (MPa)	Strand Path	Level of Prestress
SDN-40	40	Draped	Not prestressed
SSP-40	40	Straight	$0.62f_{pu}$
SDP-40	40	Draped	$0.62f_{pu}$

Table 3. Pre-stress effect.

Status	Specimens	
	Canter line deflection at pre-stress stage , mm	
	SDP-40	SSP-40
Experimen	0.91	1.25
Calculated	--	1.31
F.E.	0.93	1.29

Table 4. Comparison of the failure load.

Specimen	Failure Load, kN		$\frac{(P_u)_{FE_u}}{(P_u)_{Exp}}$
	$(P_u)_{FE}$	$(P_u)_{Exp}$	
SDN-40	135	122	1.11
SDP-40	250	240	1.04
SPP-40	175	165	1.06

.